A Knowledge-Based Analysis of Inter-Laminar Faults for Condition Monitoring of Magnetic Cores with Predominant Focus on Axial off-set Between the Fault Points

Hamed Hamzehbahmani, *Senior member IEEE*, Ruth V. Sabariego, and Benjamin Ducharne

Abstract- **Condition monitoring and fault diagnosis of electromagnetic devices is a normal practice to prevent unpredicted downtime and catastrophic failure. In this sense, inter-laminar faults (ILFs) detection or fault diagnosis in the magnetic cores is a key objective. This paper aims to present advanced experimental measurements and numerical analysis to study influence of ILFs on soft magnetic properties of magnetic cores with Grain Oriented Electrical Steels (GOES). The predominant focus of these studies and associated analysis is ILFs with axial off-set between the short circuit points. To carry out the experimental measurements, stacks of four standard Epstein size strips of GOES were assembled. Each stack was subjected to minor ILF with axial off-set from 0 to 200 mm. The test samples were magnetised under controlled sinusoidal induction at a frequency of 50 Hz, and peak inductions of 1.1 T to 1.7 T. Impacts of each fault scenario on soft magnetic properties of the test samples was investigated by monitoring and interpreting the dynamic hysteresis loops (DHLs). In favour of supporting the practical measurements, accurate time-domain finite element (FE) models were also undertaken to reproduce the DHLs, and to visualise distribution of inter-laminar eddy currents and power loss caused by ILFs.**

Index Terms: Magnetic cores, magnetic hysteresis, fault diagnosis, inter-laminar fault, axial off-set, finite element.

NOMENCLATURE

W_{tot}	Total energy loss
W_{hys}	Hysteresis energy loss
W_{eddy}	Classical eddy current energy loss
W_{exc}	Excess energy loss
$h(t)$	Magnetic field at the surface of the lamination
$h_{hys}(t)$	Hysteresis field
$h_{eddy}(t)$	Eddy current field
$h_{exc}(t)$	Excess field
W_{dyn}	Dynamic energy loss
$h_{dyn}(t)$	Dynamic field
W_{add}	Additional energy loss
$h_{add}(t)$	Additional field
$g_{dyn}(B)$	Polynomial function to control shape of DHL
δ	Directional parameter
α_{dyn}	Variable to determine frequency law of W_{exc}
$k_{add}(B)$	Polynomial function to control shape of DHL
$a(t)$	Magnetic vector potential (MVP)
$a'(t)$	Test function for the MVP
$b(t)$	Magnetic flux density or induction
$j(t)$	Electric current density
n	Outer normal on the boundary
σ	Electrical conductivity

I. INTRODUCTION

ELECTROMAGNETIC devices might be subjected to a variety of different failures and faults during their lifetime. Faults of any kind, immediately influence the overall performance and efficiency of the devices, and in some cases could potentially lead to machine breakdown. To this end, there is no hesitation that fault diagnosis of electromagnetic devices must be performed at the very beginning before they lead to catastrophic breakdowns. Fault diagnosis and condition monitoring is a procedure for monitoring the operating parameters of a device to detect potential faults at the first outset. Depend on the diagnostic objective, the procedure of fault diagnosis is followed by monitoring pre-defined parameters and interpreting their physical features, e.g., temperature, power loss, magnetic field, vibration, etc. [1-2]. Advanced signal processing and data analysis are performed to translate the acquired data into information to assess quality and status of the device under test. This is consistent with condition monitoring guiding principles and definition [3]. Condition monitoring of electromagnetic devices is consistently performed by the end users to prevent unscheduled shut down and unsafe operation of the device that could lead to irreversible and irreparable failures.

Significant research has been conducted on fault diagnosis and condition monitoring of rotating machines, in particular three phase induction motors as the most popular electric motors for industry [4-6]. To this end, the main effort has been focused on stator winding, rotor bar, and bearing. Practical techniques with high accuracy are commercially available to identify these kinds of defects, among them Motor Current Signature Analysis (MCSA) also known as Stator Current Signature Analysis (SCSA), as a reliable diagnostic technique, can be highlighted [7]. With regard to power transformers, research and development has been widely undertaken for fault diagnosis in the winding, tap changer, bushings, and terminals [8-10]. Nevertheless, not enough attention has been paid to quality assessment and fault diagnosis of the magnetic cores, specifically for power transformers.

It is worth to highlight that, magnetic core of electromagnetic devices is the most important and the first part of the device to be constructed during the manufacturing processes. Magnetic core of electromagnetic devices has a major role in energy conversion and overall performance and efficiency of the device. Overall quality and efficient performance of any type of electromagnetic device highly depends on quality of their magnetic cores. Nonetheless, there is a major requirement to develop novel techniques of fault diagnosis and condition assessment of magnetic cores of power transformers and electrical machines. The main concern of this work is impact assessment of core faults, also known as inter-laminar faults (ILFs), in electromagnetic devices with Grain Oriented Electrical Steels (GOES), namely power transformers.

Core faults mainly refer to electrical contact or low resistance between the adjacent laminations in clamped magnetic cores. ILF problems and their impacts have been identified as a consequential hazard to the regular operation of electromagnetic devices with laminated core structure. These kinds of defects in practical magnetic cores could arise due to several reasons, for example [11-14]:

- Edge burr or degradation in insulation coating at the cut edge and around the bolt holes; this could occur throughout the magnetic cores production procedures.
- Rotor-stator rub, for rotating electrical machines, due to eccentricity.
- Vibration of loose laminations due to inappropriate clamping pressure.
- Sparking from windings due to winding failure, or loose windings.

Examples of degradation at the cut edge of a stator teeth of a 1.5 kW, 50 Hz three-phase induction motor, and stator core fault due to rotor-stator rub are shown in Figs 1 and 2, respectively.

In practical magnetic cores, it is highly likely that ILFs occur at random points with axial off-sets or displacements between the fault points in the plan of the laminations. A perspective view of magnetic core of a three-phase three-limb transformer with core faults at three different locations is shown in Fig 3. In this model, short circuit points of ILF #1 are applied on opposite sides of the central limb, while there is an axial off-set between the short circuit points of ILF #2 and ILF #3. The key objective of this work is to study the impacts of these kinds of faults.

Measuring no-load power loss of power transformers is a normal practice to assess overall quality of the magnetic core, as stated in the British standard BS EN 60076-1-2011 [15]. This test is performed at the manufacturing site as well as, during the type and routine tests. Nevertheless, with this test only overall power loss of the magnetic cores can be monitored, and it does not provide any details of the magnetising processes and power loss distribution. It is well recognised that ILFs alter the normal distribution of eddy currents and magnetic field inside the laminations and within the defected zone [16-17]. Recent research showed that the phenomenology of magnetic hysteresis and associated analysis is an accurate approach to identify and classify core faults [11], [18]. Therefore, condition assessment of the magnetising processes of the magnetic cores can be

employed as a reliable technique of condition monitoring [16]. This can be achieved by monitoring the instantaneous waveforms of magnetic field strength $H(t)$ and dynamic hysteresis loops (DHL) under specific magnetisation conditions.
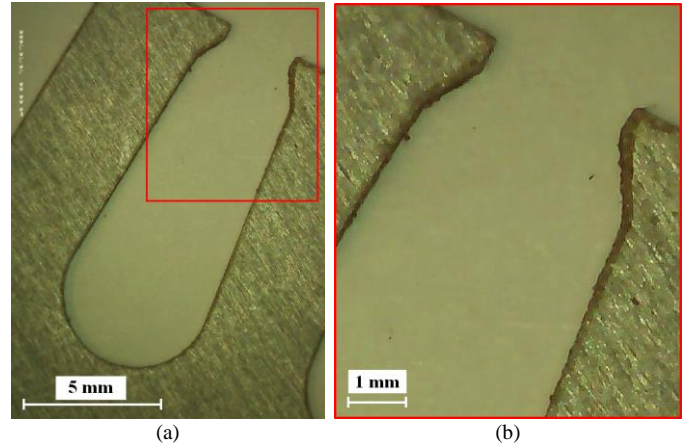

Fig 1 (a) Stator slot of a three-phase stator core (b) degradation in the insulation coating at the cut edge

Fig 2 Damage on surface of a stator core due to rotor-stator rub

The significant contribution of this work is to propose advanced experimental and numerical approaches to calculate additional magnetic field strength and additional power losses caused by ILFs. The predominant focus of this study is to assess the relation between power losses caused by ILFs and the axial off-set between the short circuits. This helps to identify the most severe faults in magnetic cores. The presented approach complies with the phenomenology of magnetic hysteresis in ferromagnetic materials. Furthermore, classical 3D FE models are presented to model ILFs and their influence on dynamic behavior of magnetic cores and localised distributions of eddy current power loss. The experimental-numerical approaches alongside the FE models can be effectively used to calculate additional eddy currents, associated magnetic fields and eventually the additional power loss due to ILFs. This provides new insight in effective condition assessment of magnetic cores of power transformers, and other electromagnetic devices constructed from GOESs.
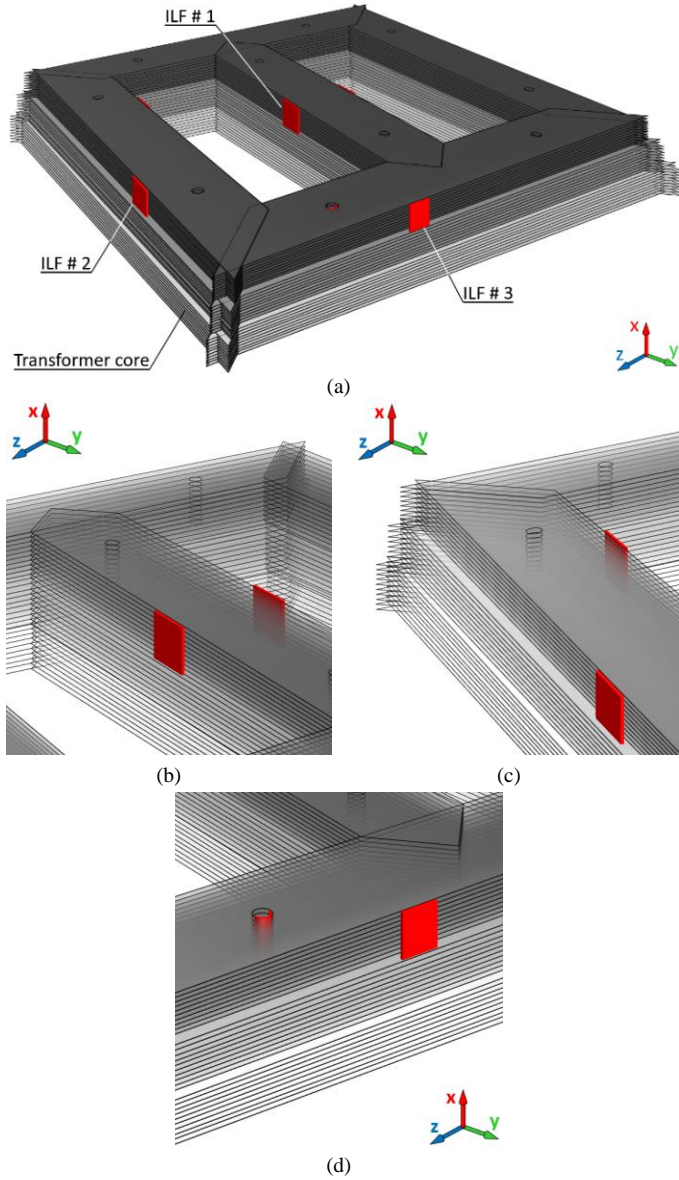
Fig 3 Perspective view of magnetic core of a three-phase transformer with ILFs (a) Overall view (b) ILF with no axial off-set (c) ILF with axial off-set on sides of a limb, and (d) ILF with axial off-set between bolt hole and yoke

II.   THEORETICAL BACKGROUND

Phenomenological concepts of magnetic hysteresis provide a solid ground to comprehend energy loss mechanism and dynamic behavior of magnetic materials. In this respect, understanding materials structure and their response to different magnetising regimes is essential. This section presents the theoretical background to model ILFs and their influences on magnetising processes.

A. Energy loss separation in GOESs

GOESs are widely used to construct magnetic cores of reactors, power transformers, and large turbogenerators. Dynamic performance of GOESs, with anisotropic texture and large grain structure, can be decently studied on the basis of the Thin Sheet Model (TSM) hinged on the statistical energy loss separation developed by Bertotti [4]. In this method, the total energy loss W_{tot} is separated into hysteresis loss W_{hys}, classical eddy-current loss W_{eddy}, and excess loss W_{exc} [19]:

$$W_{tot} = W_{hys} + W_{eddy} + W_{exc} \tag{1}$$

Energy loss mechanism can be further interpreted based on the magnetic fields, and hence (1) can be converted into magnetic field separation:

$$\underline{h}(t) = \underline{h}_{hys}(t) + \underline{h}_{eddy}(t) + \underline{h}_{exc}(t) \tag{2}$$

where $\underline{h}(t)$ is the magnetic field at the surface of the lamination, $\underline{h}_{hys}(t)$ is hysteresis field, $\underline{h}_{eddy}(t)$ is classical eddy-current field, and $\underline{h}_{exc}(t)$ is excess field.

Magnetic hysteresis is a complex phenomenon, nevertheless, in recent research it was experimentally and analytically demonstrated that ILFs make the magnetising processes even more complicated [11], [18]. Consequently, depends on fault severity, magnetising regime and DHL of a magnetic core subjected to ILF are different from the inherent properties of the materials, e.g. what could be measured for a single strip lamination. The first and the most obvious effect of ILFs is development of additional eddy current loops within the defected laminations. The circulating eddy currents change the normal magnetising processes and claim for additional magnetic field strength, which increase both localised and overall power losses. Therefore, (1) and (2) can be further developed to represent the additional energy loss W_{add} and associated magnetic field $\underline{h}_{add}(t)$ caused by ILFs [18]:

$$W_{tot} = W_{hys} + W_{eddy} + W_{exc} + W_{add} \tag{3}$$

$$\underline{h}(t) = \mathcal{H}_{hys}(\underline{b}) + \underline{h}_{eddy}(t) + \underline{h}_{exc}(t) + \underline{h}_{add}(t) \tag{4}$$

In certain analysis, analytical modelling is exclusively performed to understand dynamic behaviour of the materials. In these applications, a two components loss model is more convenient. This modelling is executed by separating the total energy loss and associated magnetic field into hysteresis and dynamic components [11], [19]:

$$W_{tot} = W_{hys} + W_{dyn} \tag{5}$$

$$\underline{h}(t) = \mathcal{H}_{hys}(\underline{b}) + \underline{h}_{dyn}(t) \tag{6}$$

Based on the two-term model, (3) and (4) yield:

$$W_{tot} = W_{hys} + W_{dyn} + W_{add} \tag{7}$$

$$\underline{h}(t) = \mathcal{H}_{hys}(\underline{b}) + \underline{h}_{dyn}(t) + \underline{h}_{add}(t) \tag{8}$$

Considering the hysteresis and dynamic magnetic fields of the two-term model as the basis of this modelling, (8) yields [18]:

$$H(t) = H_{hys}(B) + g_{dyn}(B)\delta \left|\frac{dB}{dt}\right|^{\alpha_{dyn}(B_{pk})} + k_{add}(B)\frac{dB}{dt} \tag{9}$$

where $\delta = \pm 1$ for ascending and descending branches of the hysteresis loop. The exponent $\alpha_{dyn}(B_{pk})$ designates the frequency dependence of excess loss component, and $g_{dyn}(B)$ and $k_{add}(B)$ are polynomial functions of the flux density B to control overall shape of the modelled DHL [18], [19]. Accuracy of the expanded TSM (9) for dynamic modelling of stacks of laminations subjected to ILFs has been proved in a recent publication [18].

B. Finite element model

The eddy-current problem in the lamination stack (with or without ILFs) is modeled by the classical magnetic vector potential (MVP, $\underline{a}$) formulation with magnetic induction $\underline{b} = \mathrm{curl}\,\underline{a}$ and induced current density $\underline{j} = -\sigma\partial_t\underline{a}$ (conductivity σ). It reads [20]:
Find $\underline{a}$ such that,

$$(\mathcal{H}(\underline{b}), \mathrm{curl}\,\underline{a}')_{\Omega} + (\sigma\,\partial_t\underline{a}, \underline{a}')_{\Omega_c} + \langle \underline{n} \times \underline{h}, \underline{a}' \rangle_{\Gamma} = 0 \,, \ \forall \underline{a}' \quad (10)$$

with $\underline{a}'$ a suitable test function; $\mathcal{H}(\underline{b})$ the characteristic material law (linear, nonlinear hysteretic or not); $\underline{h}$ is the field (imposed) at boundary Γ; $(\cdots, \cdots)\Omega$ and $< \cdots, \cdots > \Gamma$ denote, respectively, a volume integral in the computational domain Ω and a surface integral on its boundary Γ of the scalar product of the two arguments. The laminations and the ILFs (when present) belong to Ω_c the conducting part of Ω where induced currents appear.

Each lamination is explicitly modelled and sufficiently finely meshed along its thickness. The MVP $\underline{a}$ is discretized with edge elements, as well as and test function $\underline{a}'$, adopting a Galerkin approach [20]. Uniqueness of MVP $\underline{a}$ is ensured by a co-tree gauge condition in the non-conducting part of the computational domain [21]. We adopt a Jiles-Atherton vector hysteresis model for $\mathcal{H}(\underline{b})$ [22]. The Newton-Raphson method was employed to solve the set of nonlinear algebraic equations obtained after space and time discretisation of model (5).

III. EXPERIMENTAL TEST SETUP

In practical magnetic cores, it is highly likely that ILFs occur at random points with axial off-sets or displacements between the short circuit points in the plan of the laminations. As the key objective of this work, impacts of these faults were studied. Experimental work and numerical analysis were carried out on standard Epstein size laminations of 0.3 mm thick with standard grades of M105-30P CGO 3 wt % SiFe with a measured resistivity of $\rho = 0.461\,\mu\Omega\text{m}$. Stacks of four laminations were put together and tagged to study a range of defects with axial off-set from 0 to $200\,mm$, as shown in Table I.

Following recent experience [18], ILFs of $10\,mm$ wide and ~500 µm thick were artificially introduced using lead-free solder (resistivity $\rho = 0.13\,\mu\Omega\text{m}$). Experimental results of Stack #1, with zero off-set as the most sever fault, and Stack #7 with no ILF were used as reference to evaluate other stacks. Perspective views of these two stacks are shown in Figs 4-a and

4-b, respectively. A perspective view, side, and top views of the test samples with axial off-set are also shown in Figs 5-a to 5-c, respectively. A top view image of one of the test samples, Stack #4 with axial off-set of $60\,mm$, is also shown in Fig 6.

Table I Test samples with ILFs with axial off-set

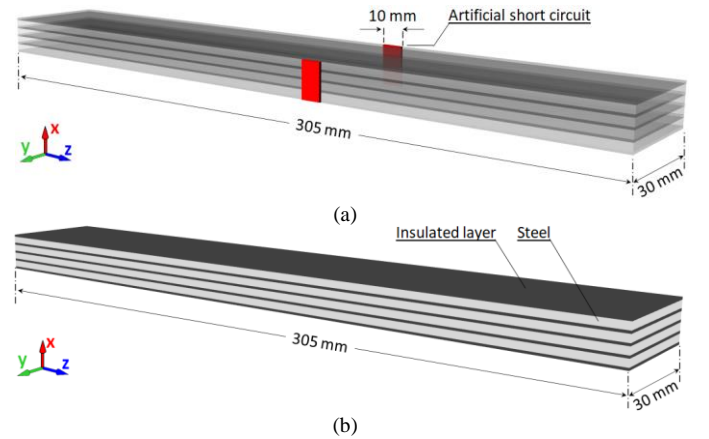| Stack Number	Axial offset $z\,(mm)$
Stack #1	0
Stack #2	20
Stack #3	40
Stack #4	60
Stack #5	100
Stack #6	200
Stack #7	No ILF

(a)

(b)

Fig 4 Perspective view of stacks of four laminations (a) without ILF (Stack #1) and (b) with ILFs at zero off-set (Stack #7)
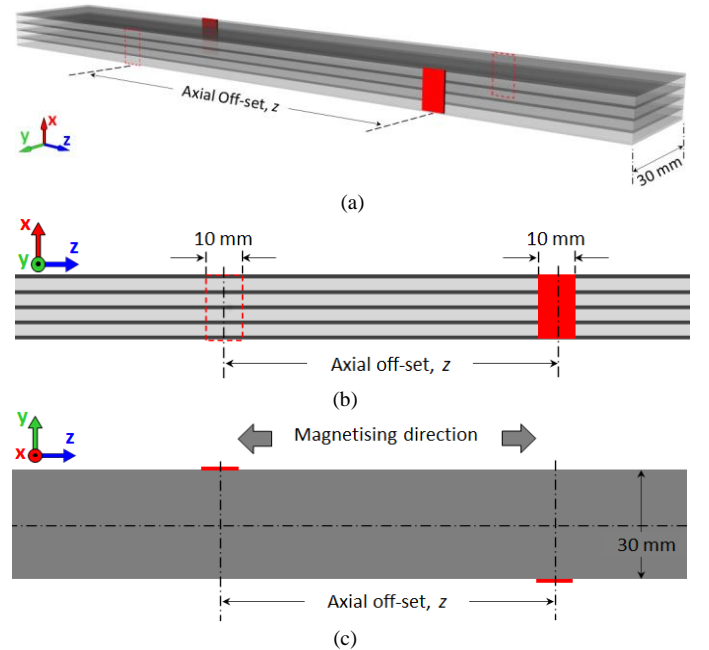

(a)

(b)

(c)

Fig 5 Perspective view (b) side view and (c) top view of stacks of four laminations axial off-set between the fault points
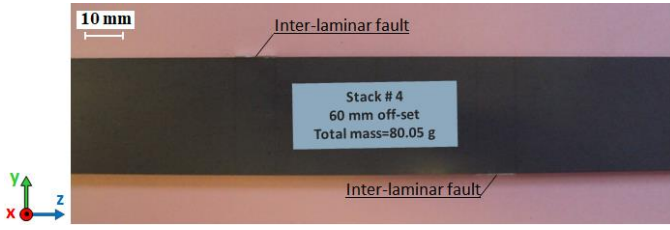
Fig 6 Top view image of Stack #4 with 60 mm off-set

In accordance with the British standard BS EN 10280:2007 [23] each stack was magnetised using a computer-controlled magnetising system [24]. A double yoke single sheet tester (SST) with $N_1 = 865$ and $N_2 = 250$, as primary and secondary winding turns, was used as the magnetising sensor; a perspective view of the SST with detailed dimensions is shown in Fig 7.
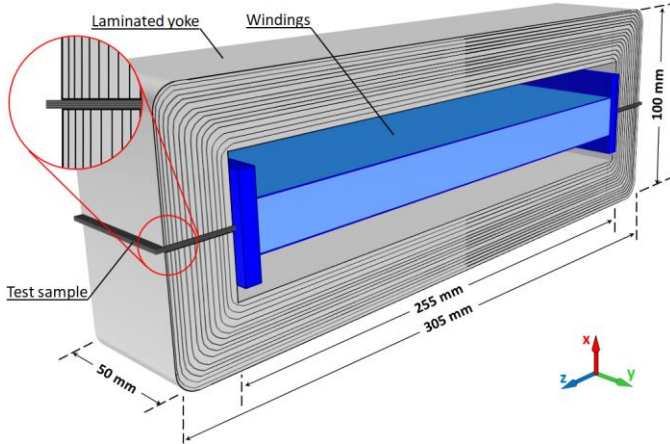

Fig 7 Schematic view of a double yoke SST used in the magnetising system

IV. EXPERIMENTAL RESULTS

In the first part of this study DHLs of the test samples were measured using the magnetising system described in section III. The results for the test samples with axial off-set from 0 to 200 mm at peak flux densities of 1.7 T, 1.5 T, 1.3 T and 1.1 T and magnetising frequency of 50 Hz are shown in Figs 8-a to 8-d, respectively. Fig 8 clearly shows that the area enclosed by the DHLs, which represents the specific energy loss per cycle, is expanded by reducing the axial off-set between the fault points. These results imply the influence of ILFs on hysteresis behavior and dynamic performance of the test samples. More precisely, magnetic hysteresis reacts to this fault by expanding the DHL area and thereby leading to increase in total energy loss. Following these measurements and to make a better indication on the results, coercivity H_c and total energy loss W_{tot} of the test samples were calculated from the measured DHLs; the results are shown in Figs 9 and 10, respectively. As an essential finding of this experiment, it was observed that H_c and W_{tot} of the test samples decline by rising the axial off-set between the short circuit points. The highest coercivity and energy loss were observed for Stack #1 with $z = 0$ mm, and they are notably reduced by increasing the axial off-set. More importantly, these quantities approached the values associated with Stack #7, when the axial off-set reached 100 mm and above.
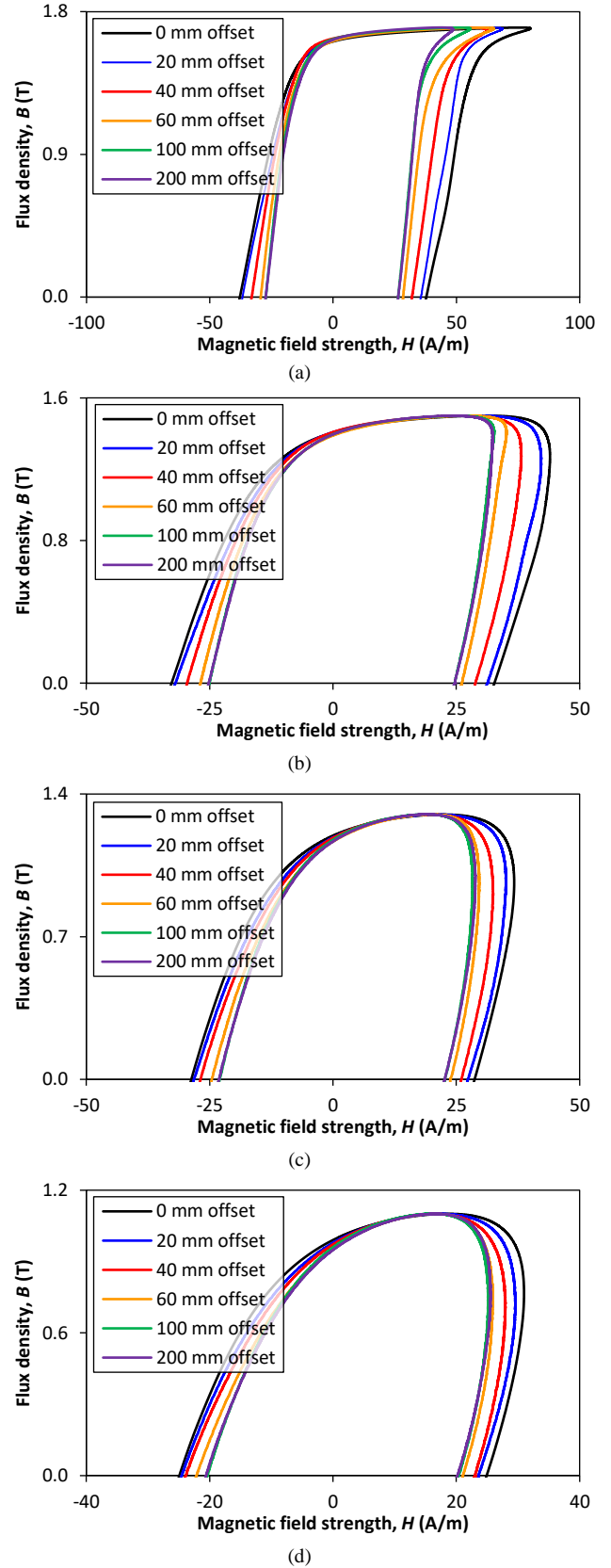

(a)

(b)

(c)

(d)

Fig 8 DHLs of the test samples measured at a magnetising frequency of 50 Hz, and peak flux densities of
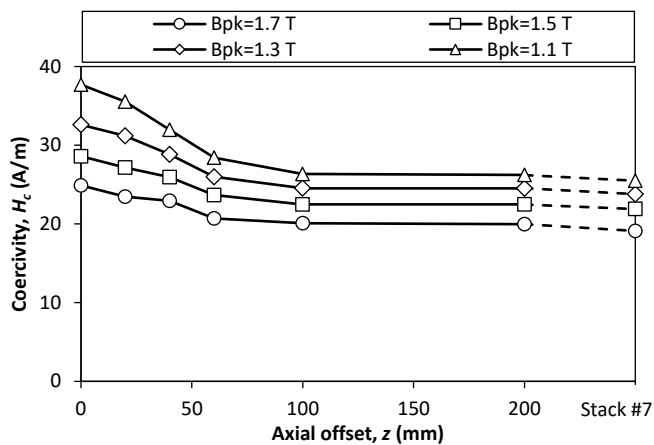(a) $B_{pk} = 1.7\ T$, (b) $B_{pk} = 1.5\ T$, (c) $B_{pk} = 1.3\ T$ and (d) $B_{pk} = 1.1\ T$

Fig 9 Measured coercivity of the test samples at power frequency of 50 Hz and peak flux densities from $B_{pk} = 1.1\,T$ to $B_{pk} = 1.7\,T$
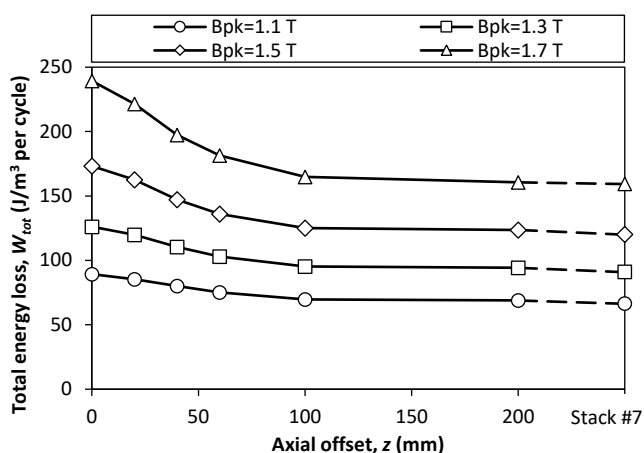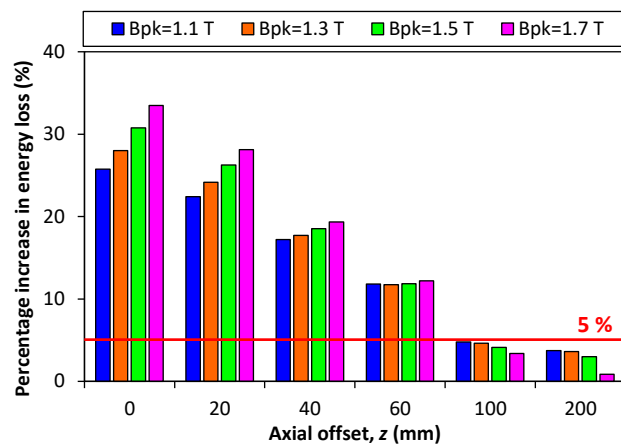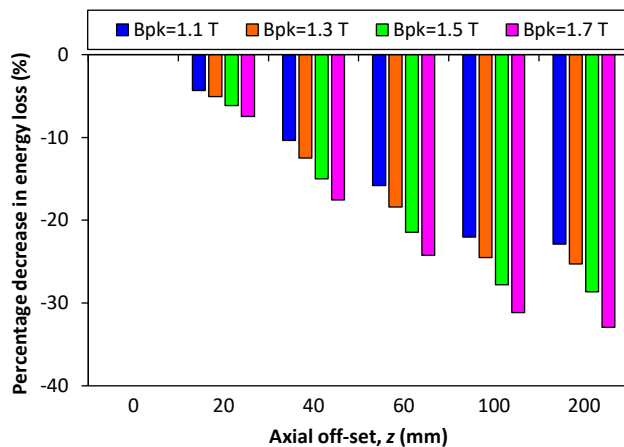

Fig 10 Total energy loss of the test samples at power frequency of 50 Hz and peak flux densities from $B_{pk} = 1.1\,T$ to $B_{pk} = 1.7\,T$

(a)

(b)

Fig 11 (a) Percentage increase in total loss of each stack compared to Stack #7, and (b) Percentage decrease in total loss of each stack compared to Stack #1

In order to illustrate the influence of ILFs on the characteristics of test samples, percentage increase in the total energy loss of each stack compared to that of Stack #7 was calculated. Percentage decrease in total energy loss of each stack with respect to that of Stack #1, was also calculated; the results for the range of measured flux densities are shown in Figs 11-a and 11-b, respectively. IEEE Std. 62.2-2004 [25] suggests that core faults, which give rise to 5 % increase in total magnetic loss (or lead to a hot spot of 10° C above the ambient after 2 hours magnetisation), should be classified as critical faults. This threshold is highlighted by a solid line on Fig 11-a. This analysis also suggests that percentage decrease of total energy loss is dramatically increased by deviating the short circuit points, as shown in Fig 11-b. This phenomenon is directly associated with the resistance of the eddy current loop created by the short circuit points on either side of the test samples. By deviating the axial off-set between the short circuit pints, effective resistance of the eddy current loop increases which results in lower ILF current and lower additional energy loss. This is evidenced by monitoring and evaluating the DHLs. As a precaution, the magnetic core or, where possible, the defected part needs to be renewed urgently.

The highest rise in energy loss was recorded for Stack #1 at a peak flux density of 1.7 T, which is 33.49 %. As a key conclusion of this experiment, it was observed that when the axial offset reached $y = 100\,mm$, the percentage increase in total energy loss falls below the threshold level of 5 % as defined in IEEE Std. 62.2-2004. Therefore, ILFs with long off-set between the shorted points cannot be of high risk for the magnetic cores and associated electromagnetic devices. Similar conclusion was previously conducted based on bulk power loss measurements [26]. This offers a reliable platform to classify ILFs and to assess their impacts on overall quality of electromagnetic apparatus with laminated core structure. This approach and associated analysis could be implemented as a powerful technique in effective condition monitoring and fault diagnosis of the magnetic cores of practical electromagnetic devices e.g., power transformers and electrical machines.

V.   NUMERICAL MODELLING

Magnetic characteristics of the test samples, including DHLs and distribution of eddy current power loss, were modelled using the numerical model, as explained in section II.B. In the FE model only 2 laminations were simulated, taking advantage

of the symmetry planes. Accordingly, for Stack #1 one-eighth of the geometry, and for other stacks half of the geometry was considered. The FE discretisation of the test samples yields to 46009 unknowns for Stack #1, and 172524 unknowns for other stacks. In this modelling, a frequency-domain simulation was performed using a vectorial Jiles-Atherton (J-A) model as the material law. The J-A model parameters $M_s = 1470000\ A/m$, $a = 3.6\ A/m$, $k = 10.4\ A/m$, $c = 0.03$ and $\alpha = 3.2e - 6$ were determined based on the optimisation of the Euclidean difference between measured and simulated static hysteresis loop of the samples in rolling direction (RD).

Dynamic characteristics of the test samples were primarily modelled by solving the MVP formulation, with imposed magnetic field strength in the RD, extracted directly from the experimental results of section IV. Note that there is no implementation of the control loop in the simulations. A comparison between the modelled and measured DHLs at a frequency of 50 Hz and peak flux density of 1.7 T for the test samples with axial off-set from 0 to $100\ mm$ are shown in Figs 12-a to 12-e, respectively.

Total energy losses of the test samples were then calculated from the modelled and measured hysteresis loops; the results are shown and compared in Figs 13. Although ILFs change the dynamic performance of the test samples and shape of the hysteresis loop, nevertheless, Fig 12 shows that the FE model (10) provides a fairly accurate basis for calculating the DHLs. As stated earlier in this section, the excitation field waveform was picked up from the experimental measurements and imposed as input of the FE simulation. Since the model is imperfect, this strategy is not ideal and could eventually impact on accuracy of the simulation. Also, in the FE model, the hysteresis loss is modelled based on the J-A vector model, while the eddy current and the additional losses are based on the model (10). A compensation is happening, as observed in Fig. 13 where the FE total loss consistently exceeds the experimental results. Still, an adequate consideration of the excess loss in the time domain would balance the loss distribution differently and increase the overall simulation accuracy. This model can be further developed to simulate influence of core fault on dynamic behaviour and soft magnetic properties of practical magnetic cores, e.g., power transformers and electrical machines.

In the last part of this study, a frequency-domain simulation was performed to model distribution of eddy current power loss at the defected zone. In this modelling a linear material with a relative permeability of $\mu_r = 3 \times 10^4$ was assumed. To keep consistency with the experimental work, a uniform sinusoidal magnetic field with a frequency of 50 Hz and amplitude of $30\ A/m$ was imposed in RD, which corresponds to a peak flux density of 1.7 T. The 3-D distributions of eddy current power loss for the test samples with axial off-set from 0 to $100\ mm$ are shown in Figs 14-a to 14-e, respectively. Note that for the sake of comparison a common scale was adopted for all fault scenarios, as shown in Fig 14. From these results, the maximum eddy current loss at the fault points for different off-sets were identified, the results are given in Table II.
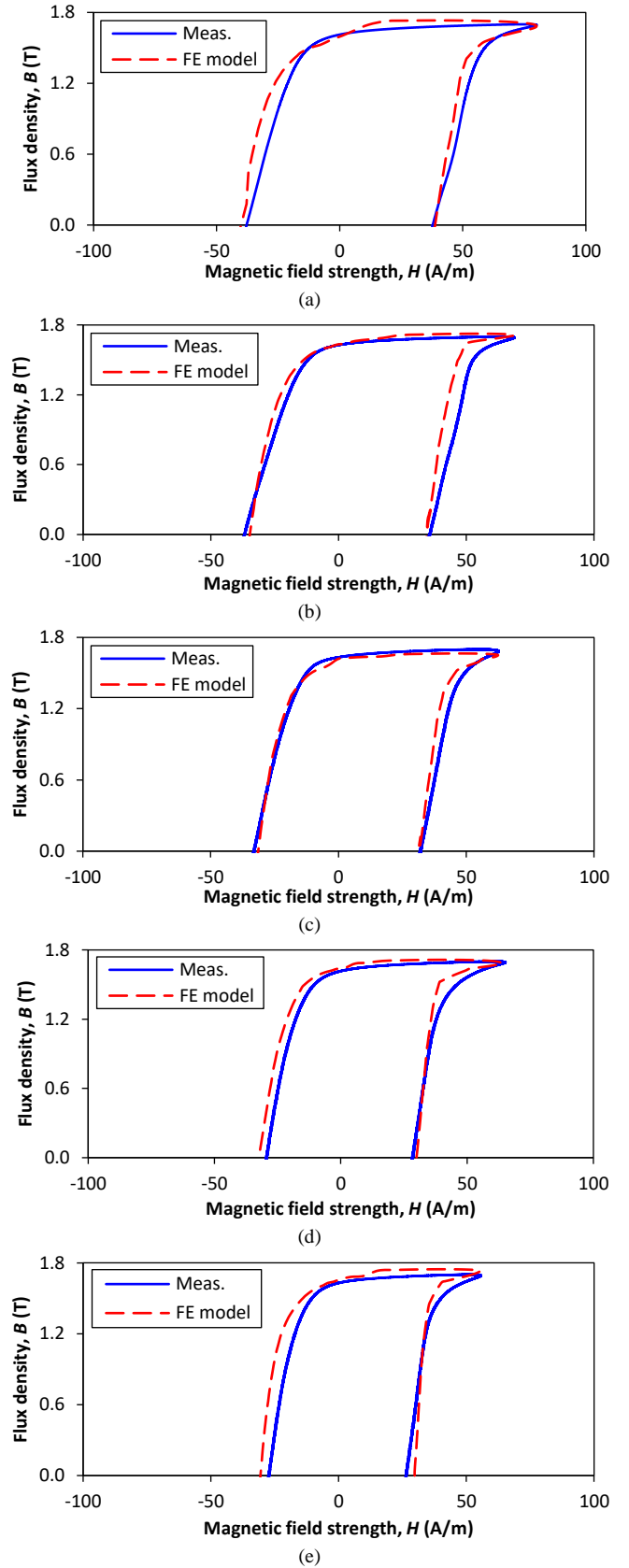

(a)

(b)

(c)

(d)

(e)

Fig 12 Comparison between the modelled and measured DHLs of the test samples at a frequency of 50 Hz and peak flux density of 1.7 T, with axial off-set of (a) 0 mm, (b) 20 mm, (c) 40 mm, (d) 60 mm and (e) 100 mm
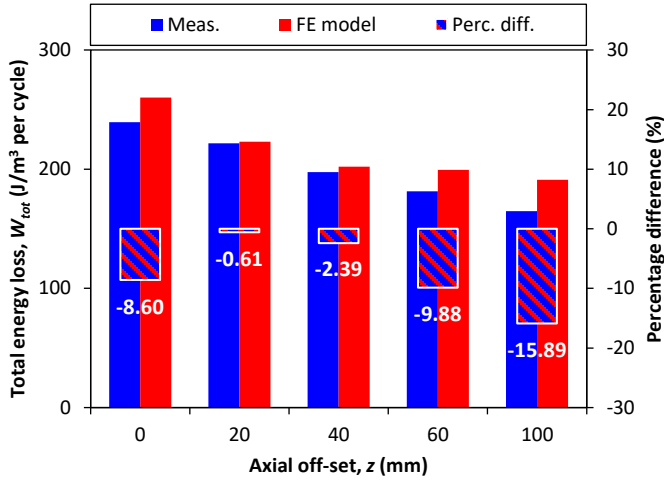
Fig 13 Comparison between the calculated and measured energy losses at a frequency of 50 Hz and peak flux density of 1.7 T

Figs 14 clearly indicates the significant impacts of ILFs on localised distribution of eddy currents and associated power losses. The results show that localised power loss at the defected zone is remarkably higher than other parts of the test samples. As expected, the highest localised power loss was observed for Stack #1 which is $10.7 \, W/kg$. It is also obvious that localised power loss reduces by increasing the axial off-set. With this configuration, localised power loss at the short circuit point was reduced to $0.810 \, W/kg$ for Stack #5 with axial off-set of $100 \, mm$. Nevertheless, as a key finding of this modelling, the results reveal that inter-laminar eddy currents spread over a wide zone between the fault points, even when axial off-set is in place. This phenomenon could be more destructive in practical magnetic cores where more laminations are involved in the ILF, which could result in high inter-laminar eddy currents faults.

It is worth to highlight that minor core faults may not necessarily be detected using the conventional techniques, e.g., overall power loss measurements. Additional localised temperature and power loss could result in insulation fatigue and consequently spread over a wider zone in the core. If not detected at the proper time, this phenomenon could continue and potentially result in irreparable failure and breakdown machine. On other word a few undetected ILFs, even with axial off-set between the short circuit points, could eventually grew and terminate into major faults. Undetected core faults could also damage the winding and culminate in inter-turn faults and ground faults.

Table II Localised eddy current power loss at the short circuit points

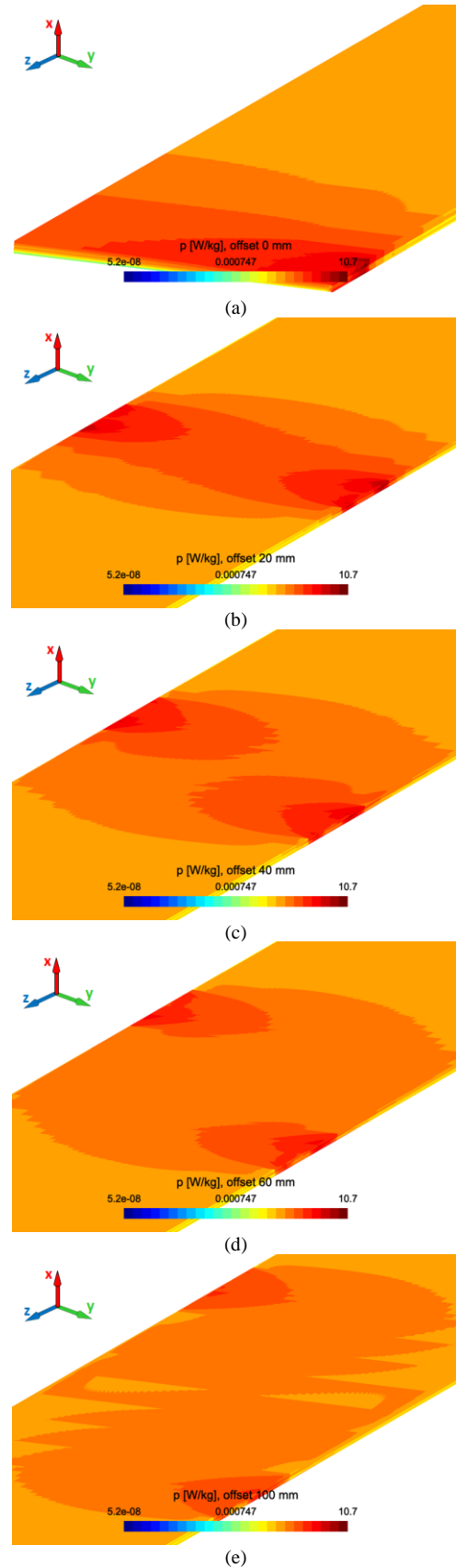| Stack Number	Axial offset z (mm)	Local eddy current loss, $P_{eddy}(w/kg)$
Stack #1	0	10.7
Stack #2	20	7.25
Stack #3	40	3.52
Stack #4	60	2.09
Stack #5	100	0.810

(a)

(b)

(c)

(d)

(e)

Fig 14 Local eddy current power loss of the test samples with axial off-set of (a) $0 \, mm$, (b) $20 \, mm$, (c) $40 \, mm$, (d) $60 \, mm$ and (e) $100 \, mm$

CONCLUSIONS

This article presents experimental measurements and time-domain FE simulations for laminated magnetic cores, exposed to ILFs. The predominant focus of this work is to study impacts of axial offset between the short circuit faults on dynamic characteristics and magnetic performance of the test samples. Experimental measurements were undertaken on stacks of standard Epstein size strips of GOESs, subjected to artificial ILFs. A standard SST was employed to monitor dynamic characteristics of each stack. DHL of each stack was measured and analysed to evaluate influence of the ILFs. Experimental results clearly showed that, phenomenology of magnetic hysteresis and analysing the dynamic characteristics of the magnetic cores is an accurate approach for quality control and condition assessment of magnetic cores. This could be implemented as a non-destructive test at the manufacturing sites, as well as during the type and routine tests of practical power transformers and electrical machines.

Time domain FE simulation were also developed to model the test samples. In this part of the work, DHL of the test samples were reproduced, and 3D distribution of eddy current power loss within the defected zone were calculated. The FE model proved to be an effective technique to evaluate influence of ILFs on eddy current and associated loss distribution within the defected zone. In fact, this modelling and associated analysis provides a new insight on influences of core failure on eddy current distribution and overall quality of the magnetic cores. This can be implemented in pre-design and design optimisation stages of magnetic cores, as well as in the condition monitoring apparatus of practical magnetic cores.

ACKNOWLEDGMENT

REFERENCES

[1] I Zamudio-Ramirez, R A Osornio-Rios, J A Antonino-Daviu, H Razik and R D J Romero-Troncoso, "Magnetic Flux Analysis for the Condition Monitoring of Electric Machines: A Review," in IEEE Transactions on Industrial Informatics, Vol. 18, No. 5, pp. 2895-2908, May 2022

[2] T Wang, G Lu and P Yan, "A Novel Statistical Time-Frequency Analysis for Rotating Machine Condition Monitoring," in IEEE Transactions on Industrial Electronics, Vol. 67, No. 1, pp. 531-541, Jan. 2020

[3] IEEE Std. C37.91, 2000 IEEE "Guide for Protective Relay Applications to Power Transformers", 2000

[4] G Bazan , A Goedtel , P Scalassara, W Endo , E Nunes , V Takase, J Guedes, and M Gentil, "An Embedded System for Stator Short-Circuit Diagnosis in Three-Phase Induction Motors Using Information Theory and Artificial Neural Networks," IEEE Transactions on Systems, Man, and Cybernetics: Systems, Vol. 52, No. 10, pp. 6582-6592, Oct. 2022

[5] H Li, Y Gu, D Xiang, P Zhang, P Yue and Y Cui, "Online Condition Monitoring of Line-End Coil Insulation for Inverter-Fed Machine by Switching Oscillation Mode Decomposition," in IEEE Transactions on Industrial Electronics, Vol. 69, No. 11, pp. 11697-11708, Nov. 2022

[6] A A Salah, D G Dorrell and Y Guo, "A Review of the Monitoring and Damping Unbalanced Magnetic Pull in Induction Machines Due to Rotor Eccentricity," in IEEE Transactions on Industry Applications, Vol. 55, No. 3, pp. 2569-2580, May-June 2019

[7] W T Thomson and I Culbert, "Current Signature Analysis for Condition Monitoring of Cage Induction Motors: Industrial Application and Case Histories", Wiley-IEEE Press, 2017

[8] S Athikessavan, E Jeyasankar, S Manohar and S Panda, "Inter-Turn Fault Detection of Dry-Type Transformers Using Core-Leakage Fluxes," in IEEE Transactions on Power Delivery, Vol. 34, No. 4, pp. 1230-1241, Aug. 2019

[9] Z Wu, L Zhou, T Lin, X Zhou, D Wang, S Gao, and F Jiang, "A New Testing Method for the Diagnosis of Winding Faults in Transformer," IEEE Transs on Instru. and Meas., Vol. 69, No. 11, pp. 9203-9214, Nov. 2020

[10] M Akbari, M Mostafaei and A Rezaei-Zare, "Estimation of Hot-Spot Heating in OIP Transformer Bushings Due to Geomagnetically Induced Current," IEEE Trans Power Deliv, vol. 38, no. 2, pp 1277-1285, April 2023

[11] H Hamzehbahmani, "A Phenomenological Approach for Condition Monitoring of Magnetic Cores Based on the Hysteresis Phenomenon," IEEE Trans. on Instru. and Meas., Vol. 70, pp. 1-9, December 2020

[12] K. Bourchas, A. Stening, J. Soulard, A. Broddefalk, M. Lindenmo, M. Dahlen and F. Gyllensten, "Quantifying effects of cutting and welding on magnetic properties of electrical steels", IEEE Trans. Ind. Appl., Vol. 53, No. 5, pp. 4269-4278, Sep./Oct. 2017

[13] M. Bali and A. Muetze, "Modelling the Effect of Cutting on the Magnetic Properties of Electrical Steel Sheets," in IEEE Transactions on Industrial Electronics, Vol. 64, No. 3, pp. 2547-2556, March 2017

[14] I Culbert and J Letal, "Signature Analysis for Online Motor Diagnostics: Early Detection of Rotating Machine Problems Prior to Failure," in IEEE Industry Applications Magazine, Vol. 23, No. 4, pp. 76-81, July-Aug. 2017

[15] BS EN 60076-1-2011, Power transformers - Part 1: General, British Standard, 2012

[16] S Hilary Nguedjang Kouakeuo, A Solignac, R Sabariego, L Morel, M Raulet, B Toutsop, P Tsafack, and B Ducharne, "Internal Characterization of Magnetic Cores, Comparison to Finite Element Simulations: A Route for Dimensioning and Condition Monitoring," in IEEE Transactions on Instrumentation and Measurement, Vol. 71, pp. 1-10, 2022, Art no. 6005310

[17] H Hamzehbahmani, P Anderson, K Jenkins and M Lindenmo, "Experimental Study on Inter-Laminar Short Circuit Faults at Random Positions in Laminated Magnetic Cores", IET Electric Power Applications, Vol. 10, Issue 7, August 2016, pp. 604–613

[18] H Hamzehbahmani, "An Enhanced Analysis of Inter-Laminar Faults in Magnetic Cores with Grain Oriented Electrical Steels for Fault Diagnosis and Condition Monitoring: Theoretical Background and Experimental Verification", IEEE Transaction on Instrumentation and Measurements, Vol. 72, pp. 1-10, March 2023, Art no. 6002610

[19] S Zirka, Y Moroz, S Steentjes, K Hameyer, K.Chwastek, S.Zurek and R Harrison "Dynamic magnetization models for soft ferromagnetic materials with coarse and fine domain structures", Journal of Magnetism and Magnetic Materials, Vol. 394, pp 229-236, Nov. 2015

[20] J Gyselinck, R V Sabariego and P Dular, "A nonlinear time-domain homogenization technique for laminated iron cores in three-dimensional finite-element models," in IEEE Transactions on Magnetics, Vol. 42, No. 4, pp. 763-766, April 2006

[21] M Pellikka, S Suuriniemi, and L Kettunen, ''Homology in electromagnetic boundary value problems,'' Boundary Value Problems, Vol. 2010, No. 1, 2010, Art. no. 381953.

[22] J Gyselinck, P Dular, N Sadowski, J Leite, and J P A Bastos, "Incorporation of a Jiles-Atherton vector hysteresis model in 2D FE magnetic field computations,", The international journal for computation and mathematics in electrical and electronic engineering, Vol. 23, No. 3, pp. 685–693, 2004.

[23] BS EN 10280:2001 + A1:2007, Magnetic Materials - Methods of measurement of the magnetic properties of electrical sheet and strip by means of a single sheet tester, British Standard, 2007

[24] H. Hamzehbahmani, P. Anderson and S. Preece "An application of an Advanced Eddy Current Power Loss Modelling to Electrical Steel in a Wide Range of Magnetising Frequency" IET Science, Measurement & Technology, Vol. 9, Issue 7, October 2015, pp. 807-816

[25] IEEE Guide for Diagnostic Field Testing of Electric Power Apparatus-Electric Machinery, IEEE Standard 62.2-2004, Jun. 2005

[26] H Hamzehbahmani, P Anderson, K Jenkins and M Lindenmo, "Experimental Study on Inter-Laminar Short Circuit Faults at Random

Positions in Laminated Magnetic Cores", IET Electric Power Applications, Vol. 10, Issue 7, August 2016, pp. 604–613

BIOGRAPHY

Hamed Hamzehbahmani (SM' 18) received the B.Eng. degree in electrical engineering from Birjand University, Birjand, Iran, in 2005, the M.Sc. degree in electrical engineering from the Iran University of Science and Technology (IUST), Tehran, Iran, in 2007, and the Ph.D. degree in electrical engineering from Cardiff University, Cardiff, U.K., in 2014. Between 2005 and 2010 he worked on distribution networks and HV substations as a consultant engineer. Following his Ph.D. he was appointed as a research associate at Cardiff University in the field of earthing systems for HVAC and HVDC systems in corporation with UK National Grid. From 2016 to 2018 he was a lecturer in electrical engineering with Ulster University in UK. He is currently an assistant professor in electrical machines and magnetic engineering at Durham University in the UK. His main research interests include magnetic materials and applications, static and dynamic modelling of magnetic materials, power loss analysis and condition monitoring of power transformers and electrical machines, high frequency and transient response analysis of earthing systems, earthing design of HVAC and HVDC networks.

Dr Hamzehbahmani is a Chartered Engineer, Member of IET, Senior Member of IEEE, and Fellow of the Higher Education Academy. He is also associate editor of IEEE Transactions on Instrumentation and Measurement, and committee member of the UK Magnetic Society.

Ruth V. Sabariego is currently associate professor with EnergyVille, Department of Electrical Engineering, KU Leuven, Belgium. She graduated in Telecommunication Engineering in 1998, University of Vigo, Spain. In October 2000, she joined the Department of Electrical Engineering and Computer Science, University of Liège, Belgium, where she obtained her PhD degree in 2004 and stayed as a post-doctoral researcher, before joining KU Leuven in October 2013.

Her expertise involves applied mathematics, computational electromagnetics with focus on model order reduction, Multiphysics, and multiscale modelling (in space and time), and the design of open-source scientific software. She is currently member of the international scientific committees of EMF, CEM. EPNC and SCEE and the editorial boards of IEEE CEFC and COMPUMAG. Since January 2020, she is an elected member of the International COMPUMAG society (ICS), a non-profit making organization serving members for the advancement of electric, magnetic or electromagnetic field computation.

She is (co-)author of some 250 peer-reviewed journal and conference papers.

Benjamin Ducharne received his MSc and PhD degrees in electrical engineering from the University Claude Bernard Lyon I, Villeurbanne, France, in 2001 and 2003, respectively. In 2004, he joined the Institute Montefiore, Liège, Belgium, where he held a post-doctoral position. In 2005, he was recruited at INSA, Lyon, France, as an Associate Professor. From 2018 to 2019, he was a Visiting Scholar and a mid-term Lecturer at Purdue University, West Lafayette, IN, USA. Since 2020, he joined ELyTMaX, Tohoku University, Sendai, Japan, as a Full-Time Researcher. His main research interests are magnetic non-destructive testing, ferromagnetic and ferroelectric materials, hysteresis modelling, fractional operators, and Multiphysics coupling.